

## Observation of the Cabibbo Suppressed Charmed Baryon Decay $\Lambda_c^+ \rightarrow p\phi$

### Abstract

We report the observation of the Cabibbo-suppressed decays  $\Lambda_c^+ \rightarrow pK^+K^-$  and  $\Lambda_c^+ \rightarrow p\phi$  using data collected with the CLEO II detector at CESR. The latter mode, observed for the first time with significant statistics, is of interest as a test of color-suppression in charm decays. We have determined the branching ratios for these modes relative to  $\Lambda_c^+ \rightarrow pK^-\pi^+$  and compared our results with theory.

The strength of color-suppression in internal W-emission charmed meson decays has long been in question. For example,  $B(D_s^+ \rightarrow \bar{K}^{*0}K^+)/B(D_s^+ \rightarrow \phi\pi^+) \simeq 1$  [1,2], while the expectation from color-matching requirements is that this ratio should be about 1/18. Reasonable overall agreement with the experimental data in the charm sector has been obtained using factorization and taking the large  $N_c$  limit in a  $1/N_c$  expansion approach, where  $N_c$  is the number of quark colors [3,4]. The Cabibbo-suppressed charmed baryon decay  $\Lambda_c^+ \rightarrow p\phi$ , shown in Figure 1, is also naively expected to be color-suppressed. However, using factorization and taking the limit  $N_c \rightarrow \infty$  leads to a prediction of no color-suppression [5]. The  $\Lambda_c^+ \rightarrow p\phi$  decay receives contributions only from factorizable diagrams, and therefore a reliable calculation should be obtained using factorization. Observation of the decay mode  $\Lambda_c^+ \rightarrow p\phi$  was first reported by the ACCMOR collaboration with  $2.8 \pm 1.9$  events [9]. Last year the E687 collaboration published results on the first observation of the Cabibbo-suppressed charmed baryon decay  $\Lambda_c^+ \rightarrow pK^+K^-$ , along with an upper limit on the resonant

substructure  $\Lambda_c^+ \rightarrow p\phi$  [10]. Herein we present new CLEO results on the observation of  $\Lambda_c^+ \rightarrow pK^+K^-$  and  $\Lambda_c^+ \rightarrow p\phi$  decays and discuss the implications of the results.

We use a data sample recorded with the CLEO II detector operating at the Cornell Electron Storage Ring (CESR). The sample consists of  $e^+e^-$  annihilations taken at and slightly below the  $\Upsilon(4S)$  resonance, for a total integrated luminosity of  $3.46 \text{ fb}^{-1}$ . The main detector components which are important for this analysis are the tracking system and the barrel Time-of-Flight (TOF) particle identification system. Additional particle ID is provided by specific ionization ( $dE/dx$ ) information from the tracking system's main drift chamber. A more detailed description of the CLEO II detector has been provided elsewhere [11].

To search for the  $\Lambda_c^+$  signals, we study  $pK^+K^-$  track combinations found by the tracking system. The  $p$  and  $K^\pm$  candidates are identified by combining information from the TOF and  $dE/dx$  systems to form a combined  $\chi^2$  probability  $\mathcal{P}_i$  for each mass hypothesis  $i = \pi, K, p$ . Using these probabilities  $\mathcal{P}_i$ , a normalized probability ratio  $L_i$  is evaluated for each track according to the formula:  $L_i \equiv \mathcal{P}_i / (\mathcal{P}_\pi + \mathcal{P}_K + \mathcal{P}_p)$ . Well-identified protons form a sharp peak near  $L_p = 1$ , while tracks identified as *not* being protons form a peak near  $L_p = 0$ . The remainder of the candidates fall in the region between 0 and 1. For the proton involved in each decay mode under study, we require  $L_p > 0.9$ , which constitutes a strong cut. For the kaons, we apply a loose cut of  $L_K > 0.1$ . In addition, all protons and kaons must pass a minimum requirement of  $\mathcal{P}_p > 0.001$  and  $\mathcal{P}_K > 0.001$ , respectively. In order to reduce the large combinatoric background, the candidate  $\Lambda_c^+$  scaled momentum  $x_p = P_{\Lambda_c} / \sqrt{E_{beam}^2 - m_{\Lambda_c}^2}$  is limited to  $x_p > 0.5$ .

The  $pK^+K^-$  invariant mass is shown in Figure 2. The broad enhancement in the mass region above  $2.37 \text{ GeV}/c^2$  is a reflection from the decay mode  $\Lambda_c^+ \rightarrow pK^-\pi^+$ , the pion has been misidentified as a kaon. The spectrum is fitted to a Gaussian for the signal with width fixed to  $\sigma = 4.9 \text{ MeV}/c^2$  determined from Monte Carlo simulation [12], and a 2<sup>nd</sup> order Chebychev polynomial for the smooth background. This fit yields  $214 \pm 50$  events for the inclusive  $\Lambda_c^+ \rightarrow pK^+K^-$  signal with a mean mass of  $2285.5 \pm 1.2 \text{ MeV}/c^2$  [13].

To find a  $\Lambda_c^+ \rightarrow p\phi$  signal, we reconstruct  $\phi$  candidates through their decays  $\phi \rightarrow K^+K^-$ . Because the width of the  $\phi$  is comparable to the detector mass resolution, the  $\phi$  signal shape is best described by a convolution of a Gaussian and a Breit-Wigner of width  $\Gamma = 4.43 \text{ MeV}/c^2$  [1]. The background is parameterized by a function of the form  $b(m) = N(m-m_0)^\alpha e^{\beta(m-m_0)}$ . The measured Gaussian resolution from the fit is  $\sigma = 1.6 \pm 0.2 \text{ MeV}/c^2$ . In order to perform background subtractions,  $1.0121 < m_{KK} < 1.0273 \text{ GeV}/c^2$  is designated as the  $\phi$  “signal” region, while  $0.990 < m_{KK} < 1.005 \text{ GeV}/c^2$  and  $1.035 < m_{KK} < 1.050 \text{ GeV}/c^2$  are designated as the “sideband” regions. Integrating the background function over the sideband and signal regions gives a signal-to-sideband scale factor  $R_\phi = 0.560 \pm 0.016$ , which is used in the  $\phi$  background subtraction below.

In order to obtain the  $\Lambda_c^+ \rightarrow p\phi$  signal, the  $pK^+K^-$  mass plot is made both for  $m_{K^+K^-}$  in the  $\phi$  signal region and the  $\phi$  sideband regions. Figure 3 shows the results. The spectra are fitted to a Gaussian for the signal with width fixed to  $\sigma = 4.9 \text{ MeV}/c^2$  from Monte Carlo, and a 2nd order Chebychev polynomial for the smooth background. The fit to the  $pK^+K^-$  mass spectrum corresponding to the  $\phi$  signal region yields  $54 \pm 12$  events with a confidence level of 97%. The mean mass for the signal is measured to be  $2288.2 \pm 1.3 \text{ MeV}/c^2$ . In fitting the  $pK^+K^-$  mass corresponding to the  $\phi$  sideband region, the mean  $\Lambda_c^+$  mass is fixed to that obtained from the  $\phi$  signal region and the  $\sigma$  is fixed to the Monte Carlo value as before. This gives  $-16.4 \pm 9.6$  events for the  $\phi$ -sideband  $\Lambda_c^+$  yield. Since the true contribution must be positive-definite, we set the central value to zero and use  $0. \pm 9.6$  as the best estimate of the  $\Lambda_c^+ \rightarrow pK^+K^-$  contribution. After scaling this by  $R_\phi$  and subtracting, we find that the net  $\Lambda_c^+ \rightarrow p\phi$  yield is  $54 \pm 13$  events. This gives  $-16.4 \pm 9.6$  events for the  $\phi$ -sideband  $\Lambda_c^+$  yield. Since the true contribution must be positive-definite, we set the central value to zero and use  $0. \pm 9.6$  as the best estimate of the  $\Lambda_c^+ \rightarrow pK^+K^-$  contribution. After scaling this by  $R_\phi$  and subtracting, we find that the net  $\Lambda_c^+ \rightarrow p\phi$  yield is  $54 \pm 13$  events. [ *NOTE TO CLEO READERS: Please See the CLEO Appendix at the end of this document.*]

As a check of the non-resonant contribution to the  $\Lambda_c^+ \rightarrow p\phi$  signal, we fit the  $K^+K^-$  mass spectra corresponding to the  $\Lambda_c^+$  signal and sideband regions as determined from the

inclusive  $pK^+K^-$  mass spectrum. The  $\phi$  yield obtained from the  $\Lambda_c^+$  sideband regions,  $2.246 < m_{pKK} < 2.266$  and  $2.306 < m_{pKK} < 2.326$  GeV/ $c^2$ , is subtracted from that for the  $\Lambda_c^+$  signal region,  $2.276 < m_{pKK} < 2.296$  GeV/ $c^2$ . Figure 4 shows the fits to the  $K^+K^-$  spectra from the  $\Lambda_c^+$  signal and sideband regions, which yield  $\phi$  signals of  $92.2 \pm 17.0$  events and  $36.5 \pm 13.5$  events, respectively. The  $\Lambda_c^+$  sideband  $K^+K^-$  mass spectrum in the Figure 4 has been scaled by the  $\Lambda_c^+$  signal-to-sideband scale factor of  $R_{\Lambda_c^+} = 0.502 \pm 0.013$ , obtained by integrating the background function in Figure 2 over the  $\Lambda_c^+$  signal and sideband regions. This gives  $56 \pm 22$  events for the  $\Lambda_c^+ \rightarrow p\phi$  signal, which is in agreement with the first method.

A check is also made for a possible reflection from  $D_s^+ \rightarrow \phi\pi^+$ , where the pion is misidentified as a proton. It is found that the reflection is a broad enhancement in the mass region above the signal. The effect of this background is minimized by the tight particle-ID requirement on the proton. Consequently, the overall fake rate is less than 1%, causing negligible effect on the  $\Lambda_c^+ \rightarrow p\phi$  signal yield from the fit.

The decay  $\Lambda_c^+ \rightarrow pK^-\pi^+$  is used as the normalization mode for the  $\Lambda_c^+ \rightarrow p\phi$  relative branching ratio. In finding the  $\Lambda_c^+ \rightarrow pK^-\pi^+$  yield, the same cuts are applied as in the  $\Lambda_c^+ \rightarrow pK^+K^-$  analysis to minimize systematic errors, except that the particle-ID for the  $\pi^+$  is loosened to a consistency requirement:  $\mathcal{P}_\pi > 0.001$ . The  $\Lambda_c^+ \rightarrow pK^-\pi^+$  mass spectrum is shown in Figure 5. The parameterization of the fit is the same as the  $\Lambda_c^+ \rightarrow p\phi$  mass fit in Figure 3, except that the width of the Gaussian is allowed to vary. The fit yields  $5683 \pm 138$  observed signal events with a mean of  $2286.8 \pm 0.2$  MeV/ $c^2$  and a width of  $6.4 \pm 0.2$  MeV/ $c^2$ . If the width of the Gaussian is fixed to the Monte Carlo prediction of 5.8 MeV/ $c^2$ , the yield changes by 4%. This dependence is included in the systematic error.

Monte Carlo simulation is used to determine all aspects of the detection efficiency except particle-ID. The particle-ID efficiency for protons is obtained using a sample of 33000  $\Lambda \rightarrow p\pi^-$  decays with a signal-to-background ratio of 50:1 [16]. For protons thus identified, the momentum spectrum after the particle-ID cuts ( $L_p > 0.9$ ,  $\mathcal{P}_p > 0.001$ ) is divided by the momentum spectrum before these cuts, bin by bin, yielding the particle-ID efficiencies versus momentum. To calculate the detection efficiency, the measured efficiency is folded in

by randomly rejecting the corresponding fraction of Monte Carlo tracks in each momentum bin. The particle-ID ( $L_K > 0.1$ ,  $\mathcal{P}_K > 0.001$ ) efficiency for the kaons is derived in an analogous manner, except that the kaons are taken from  $D^*$  decays through the cascade process  $D^{*+} \rightarrow D^0\pi^+$ ,  $D^0 \rightarrow K^-\pi^+$ . A sample of 11000 such  $D^0 \rightarrow K^-\pi^+$  decays is obtained with an 8:1 signal-to-background ratio [16]. The particle-ID efficiency for protons is near 90% from 300 MeV/c<sup>2</sup> to 1.1 GeV/c<sup>2</sup> falling off to below 10% by 2.5 GeV/c<sup>2</sup>. For kaons the particle-ID efficiency remains relatively flat at about 95%.

Using a Monte Carlo sample of  $\Lambda_c^+ \rightarrow p\phi$  decays, where the  $\Lambda_c^+$  fragmentation takes place according to the Lund JETSET Monte Carlo [17], the full detection efficiency is determined, with the particle-ID portion folded in as described above. For  $\Lambda_c^+ \rightarrow p\phi$ , the overall efficiency is  $0.178 \pm 0.004$  including the particle-ID efficiency which is  $0.425 \pm 0.011$ . For  $\Lambda_c^+ \rightarrow pK^+K^-$  (non-resonant) and  $\Lambda_c^+ \rightarrow pK^-\pi^+$  the overall efficiencies are  $0.216 \pm 0.005$  and  $0.224 \pm 0.005$ , respectively.

Since for all the decay modes the requirement  $x_p > 0.5$  is applied, the relative branching ratio for each mode is found simply by dividing the corrected yields. Table I gives the details, listing only the statistical errors. The  $\phi \rightarrow K^+K^-$  branching ratio is explicitly included in the calculation of the  $\Lambda_c^+ \rightarrow p\phi$  branching ratio, and its uncertainty is included in the systematic errors.

The estimates for the main sources of systematic error include the  $\Lambda_c^+ \rightarrow p\phi$  and  $\Lambda_c^+ \rightarrow pK^+K^-$  signal shapes (7% and 11%, respectively) and background shapes (2% and 10%, respectively), particle-ID efficiency (6%), and the  $\Lambda_c^+ \rightarrow pK^-\pi^+$  fit (4%). In addition, for the  $\Lambda_c^+ \rightarrow p\phi$  mode, varying the  $\phi$  signal and sideband regions gives a 5% variation in the yield. Finally, there is a 1.8% contribution to the  $\Lambda_c^+ \rightarrow p\phi$  systematic error from the  $\phi \rightarrow K^+K^-$  branching ratio uncertainty. Thus we estimate 12% systematic error in  $B(p\phi/pK\pi)$ , 17% in  $B(pKK/pK\pi)$ , and 18% in  $B(p\phi/pKK)$ . The final results appear in Table II, along with those from NA32 [9] and E687 [10]. Also shown in the table are theoretical predictions from Cheng and Tseng [5], Körner and Krämer [6], Żenczykowski [7], and Datta [8].

In summary, we have observed the Cabibbo-suppressed decays  $\Lambda_c^+ \rightarrow p\phi$  and  $\Lambda_c^+ \rightarrow pK^+K^-$ . The results appear in Table II, which show that the phenomenological treatments of the  $\Lambda_c^+ \rightarrow p\phi$  decay rate agree within a factor of two or three with our result. Since naive color suppression arguments would have required a  $\Lambda_c^+ \rightarrow p\phi$  decay rate much smaller (by a factor of about 15), our result suggests, at least for the factorizable diagrams, that color-suppression is inoperative in charm baryon decays [5]. Furthermore, within the factorization approach using a  $1/N_c$  expansion, our result supports the validity of taking the large  $N_c$  limit in charm baryon decays.

---

- [1] Particle Data Group, L. Monatet *et al.* Phys. Rev. D **50**, 1173 (1994).
- [2] Unless otherwise specified, reference to a state also implies refernce to the charge conjugate state.
- [3] A. J. Buras, J.-M. Gérard, and R. Rückl, Nuc. Phys. **B268**, 16 (1986).
- [4] M. Bauer, B. Stech, and M. Wirbel, Z. Phys. C **34**, 103 (1987).
- [5] H. Cheng and B. Tseng, Phys. Rev. D **46**, 1042 (1992).
- [6] J.G. Körner and M. Krämer, Z. Phys. C **55**, 659 (1992).
- [7] P. Żenczykowski, Phys. Rev. D **50**, 402 (1994).
- [8] A. Datta, UH-511-824-95, April 1995.
- [9] S. Barlag *et al.*, Z. Phys. C **48**, 29 (1990).
- [10] P.L. Frabetti *et al.*, Phys. Lett. B 314, 477–481 (1993).
- [11] Y. Kubota *et al.*, Nucl. Instrum. Methods **A320**, 66–113 (1992).
- [12] The Monte Carlo employs the CERN GEANT package:

R. Brun *et al.*, GEANT 3.14, CERN DD/EE/84-1.

[13] The quoted uncertainties in mass measurements refer to statistical error only.

[14] The remaining background is removed by sideband subtraction.

[15] T. Sjöstrand, *Comp. Phys. Comm.*, **43** 367 (1987).

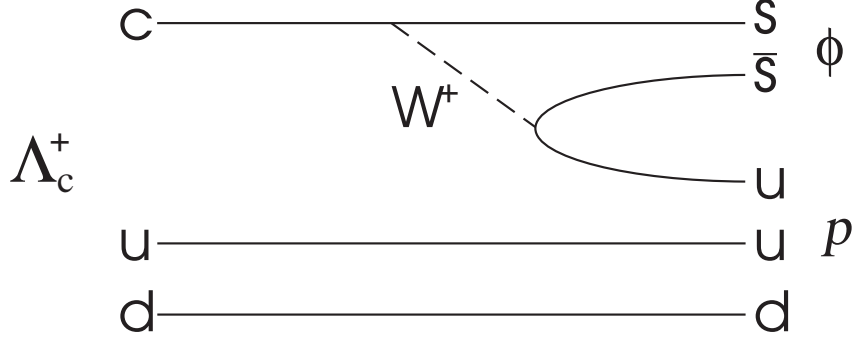


FIG. 1. The decay  $\Lambda_c^+ \rightarrow p\phi$ .

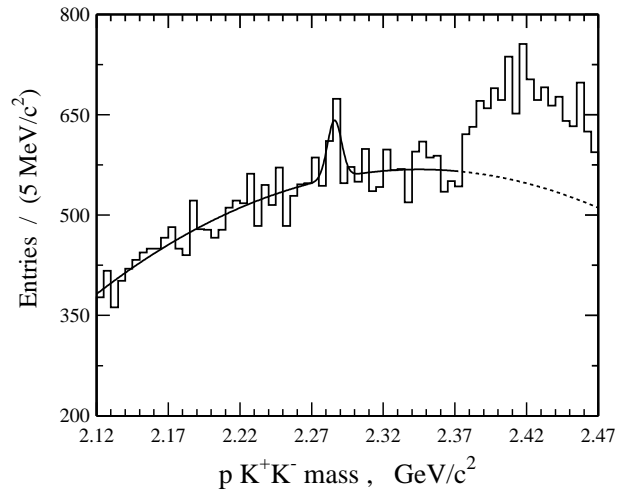


FIG. 2. Invariant mass of inclusive  $pK^+K^-$  combinations passing all requirements. No  $\phi$  cut is applied. The region above  $2.37 \text{ GeV}/c^2$ , where there is a large enhancement from  $\Lambda_c^+ \rightarrow pK^-\pi^+$  decays, is not included in the fit.

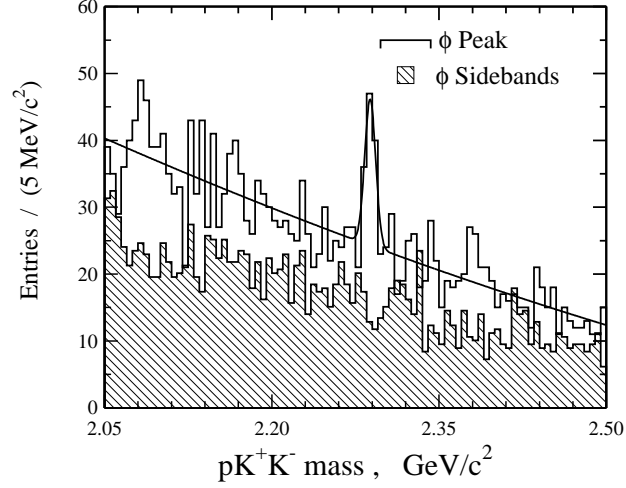


FIG. 3. Invariant mass of  $pK^+K^-$  combinations corresponding to  $K^+K^-$  mass in the  $\phi$  “signal” (unshaded) and “sideband” (shaded) regions.

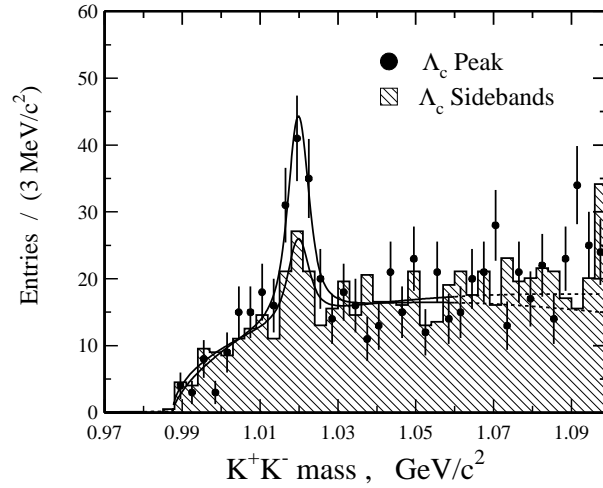


FIG. 4. Fit to  $K^+K^-$  mass from combinations belonging to the  $\Lambda_c^+$  signal (unshaded) and sideband (shaded) regions. The region above 1.06  $\text{GeV}/c^2$  is not included in the fit because of  $K^{*0}$  feed-up when the  $\pi$  is misidentified as a  $K$ .

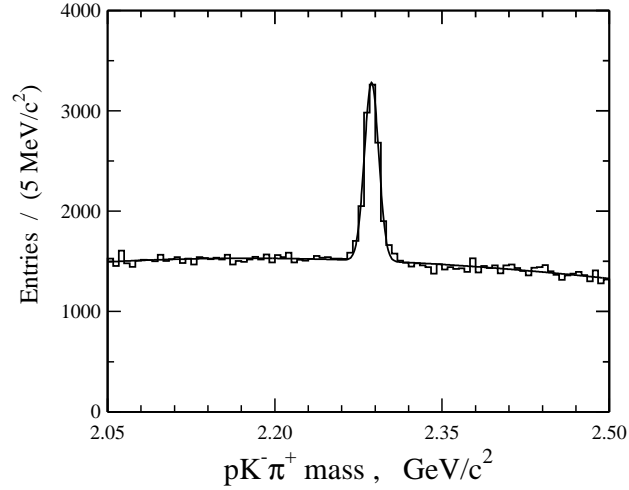


FIG. 5. Invariant mass of  $pK^-\pi^+$  combinations found in the same data sample. The  $\Lambda_c^+ \rightarrow pK^-\pi^+$  signal is used for normalization of the  $\Lambda_c^+ \rightarrow p\phi$  branching ratio.

TABLE I. Calculation of the branching ratios for  $\Lambda_c^+ \rightarrow p\phi$  and  $\Lambda_c^+ \rightarrow pK^+K^-$  relative to  $\Lambda_c^+ \rightarrow pK^-\pi^+$  and  $\Lambda_c^+ \rightarrow pK^+K^-$ . The errors are statistical only.

$\Lambda_c^+$ Decay Mode:	$\Lambda_c^+ \rightarrow p\phi$	$\Lambda_c^+ \rightarrow pK^+K^-$	$\Lambda_c^+ \rightarrow pK^-\pi^+$
Raw Yield	$54 \pm 12$	$214 \pm 50$	$5683 \pm 138$
Efficiency	$0.178 \pm 0.004$	$0.216 \pm 0.005$	$0.224 \pm 0.005$
$B(\phi \rightarrow K^+K^-)$	$0.491 \pm 0.005$		
Corrected Yield	$618 \pm 138$	$991 \pm 233$	$25371 \pm 837$
$B/B(\Lambda_c^+ \rightarrow pK^-\pi^+)$	$0.024 \pm 0.006$	$0.039 \pm 0.009$	1
$B/B(\Lambda_c^+ \rightarrow pK^+K^-)$	$0.62 \pm 0.20$	1	

TABLE II. Final results on  $\Lambda_c^+ \rightarrow p\phi$  and  $\Lambda_c^+ \rightarrow pK^+K^-$ .

Ratio of interest:	$\mathcal{B}(p\phi)/\mathcal{B}(pK\pi)$	$\mathcal{B}(pKK)/\mathcal{B}(pK\pi)$	$\mathcal{B}(p\phi)/\mathcal{B}(pKK)$
This experiment	$0.024 \pm 0.006 \pm 0.003$	$0.039 \pm 0.009 \pm 0.007$	$0.62 \pm 0.20 \pm 0.12$
NA32	$0.04 \pm 0.03$		
E687		$0.096 \pm 0.029 \pm 0.010$	$< 0.58@90\%C.L.$
Cheng & Tseng	$0.045 \pm 0.011$		
Żenczykowski	0.023		
Datta	0.01		
Körner& Krämer	0.05		